Chemical tuning of band alignments for metal gate/high-κ oxide interfaces

Y. F. Dong,[1] S. J. Wang,[2,*] Y. P. Feng,[1,†] and A. C. H. Huan[2]
[1]*Department of Physics, National University of Singapore, Singapore 117542*
[2]*Institute of Materials Research and Engineering, 3 Research Link, Singapore 117602*
(Received 1 August 2005; revised manuscript received 7 October 2005; published 3 January 2006)

We report a method for chemical tuning of band alignments for metal gate/high-κ oxide interfaces. A heterovalent metal interlayer was included between the metal gate electrode and high-κ oxide. Based on our first-principles calculations for Ni/ZrO_2(001) interfaces, a tunability as wide as 2.8 eV can be achieved for the effective work function of metal gate on high-κ oxide which far exceeds the required tuning range. In addition, we found a simple linear relationship between the effective metal work function and the electronegativity of interlayer metal atom for most of the transition metals considered. The localized interfacial dipole was found to dominate the contribution to the formation of Schottky barrier heights at metal/dielectric oxide interfaces.

DOI: 10.1103/PhysRevB.73.045302 PACS number(s): 73.30.+y, 73.20.At, 73.40.−c, 77.55.+f

I. INTRODUCTION

The continual downscaling of semiconductor devices into the "nano" era requires not only the replacement of silicon dioxide (SiO_2) gate dielectric by high dielectric constant (high-κ) materials,[1–6] but also that of polycrystalline Si (poly-Si) gate electrodes by metal gates.[7–10] In an actual metal-oxide-semiconductor field-effect transistor (MOSFET) device, it is the effective work function of metal gate ($\Phi_{m,\mathrm{eff}}$), the energy position of metal Fermi level in Si channel in flat-band condition (Fig. 1), that determines the effective confinement of carriers and the gate threshold voltage. The integration of metal gate with high-κ gate dielectric requires the effective metal work functions ($\Phi_{m,\mathrm{eff}}$) to be within ±0.1 eV of Si valence- and conduction-band edges for *p*- and *n*-channel MOSFETs, respectively.[11] However, to find two metals with suitable work functions and to integrate them with current semiconductor technology remains a challenge. In addition, selection of metal gate materials is not straightforward because the effective work function of a metal depends on the underlying gate dielectrics and could differ appreciably from the metal work function in vacuum ($\Phi_{m,\mathrm{vac}}$).[7,12] In order to identify the right metal gate material, understanding and controlling the interfaces between metal gate electrode and high-κ dielectric at the atomic scale is essential. In this paper, we propose a method for atomic-level chemical tuning of band alignment for metal gate on high-κ dielectric, which aims to provide a practical way of modifying the band alignments for metal gate/high-κ oxide interfaces to satisfy the engineering requirement for metal gate technology.

II. MODELS AND CALCULATION

Cubic ZrO_2 (c-ZrO_2) and face-centered cubic (fcc) Ni were used in our study as prototypes for high-κ dielectric gate oxides and metal gate electrodes, respectively. Ni has very good lattice match to ZrO_2 which allows fabrication of high quality metal-oxide interface. Instead of growing the metal directly on the oxide, we proposed to include a layer of heterovalent metal m (m=Au, Pt, Ru, Mo, Al, V, Zr, Ti, and W) between them. Due to different electronegativity of the heterovalent metal atoms, the interlayer is expected to change the interface electric dipole moment and result in changes in the band alignment at the metal-oxide interfaces. Chemical tuning of Schottky barrier height (SBH) and effective metal work function can be achieved by using different metals or different coverage for the interlayer.

We consider two models, one with a full monolayer of heterovalent atoms [Fig. 2(a)] and the other with half monolayer [Fig. 2(b)] between an oxygen-terminated ZrO_2 (001) surface and Ni (001). First-principles method based on the spin-polarized density functional theory (SDFT) was used to investigate the structure and properties of Ni(001)-m-ZrO_2(001) interfaces. Total energy calculations were carried out using the Vienna *ab initio* simulation package (VASP),[13,14] with Vanderbilt ultrasoft pseudopotentials,[15] and the generalized gradient approximation[16] (GGA) for exchange and correlation. A plane-wave cutoff corresponding to a kinetic en-

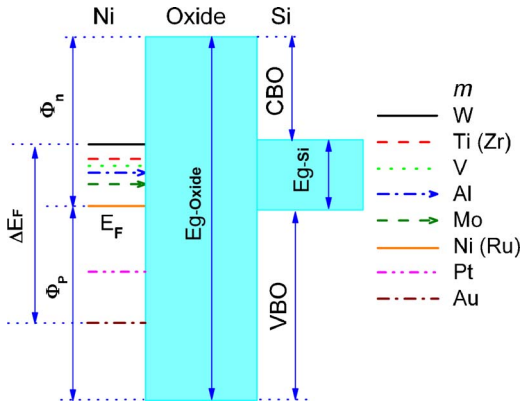

FIG. 1. (Color online) Energy band diagram of Ni-ZrO_2-Si (MOS) structures with an interlayer of heterovalent metal m between Ni and ZrO_2. The $n(p)$-type Schottky barrier height $\Phi_n(\Phi_p)$, the conduction band offset (CBO), and valence band offset (VBO), are shown. The energy positions of Fermi level for different interlayer metal m are denoted by colored lines (The lines' sequence is shown on the right side.). The tuning range (ΔE_F) of $\Phi_{m,\mathrm{eff}}$, by inserting half monolayer of heterovalent metal m between Ni and ZrO_2, is also shown.

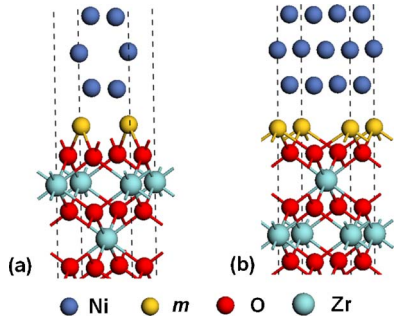

FIG. 2. (Color online) Supercells for the Ni-m-ZrO_2 interfaces, (a) with one monolayer metal m (m=Ni, V, and Al), (b) with half monolayer metal m (m=Au, Pt, Ni, Ru, Mo, Al, V, Zr, and W). The interface is formed using c-ZrO_2(001) and fcc Ni(001) surfaces, with either half or one monolayer of heterovalent metal (m) between them.

ergy of 350 eV was used. A **k** point mesh of $8\times8\times1$ was used to sample the (1×1) interface supercell (3.647 Å $\times$3.647 Å). In the plane parallel to the interface (xy plane), the lattice constant was constrained to that of bulk c-ZrO_2. The lattice constant normal to the interface (z-direction) and atomic positions were fully optimized to minimize the total energy. Density of states (DOS) were calculated with finer **k** meshes ($\sim$0.02 $Å^{-1}$) using the tetrahedron method with Blöchl corrections[17] as implemented in VASP.

III. RESULTS AND DISCUSSION

Figures 3(a) and 3(b) show the spin-resolved and atomic site-projected density of states (PDOS) of two interfaces Ni-Pt-ZrO_2 and Ni-Al-ZrO_2 with half monolayer of Pt and Al, respectively. In these and all systems being studied, the PDOS of atoms far from the interface (bulk region) are essentially the same as those in bulk fcc Ni or c-ZrO_2. But the position of the Fermi level in the band gap of bulk oxide is strongly dependant on the interfacial metal m. This indicates that inclusion of the heterovalent metal changes interface dipoles. The interface oxygen anions are noticeably perturbed by the formation of the interface, and gap states appear in the PDOS of interface oxygen. It is convenient to consider two sources for the gap states, contribution from the interfacial chemical bonds and contribution from the tails of the metallic wave functions which tunnel into the oxide band gaps or conventional metal induced gap states (MIGS).[18,19] The former is localized in the interfacial bond region, while MIGS decay exponentially inside the oxide.

To closely examine the spatial dispersion of the occupied gap states, we calculated the corresponding charge density profile along the normal direction of the interface

$$\rho(z) = A^{-1}(E_F - E_{\mathrm{VBM}})^{-1}\int_{E_{\mathrm{VBM}}}^{E_F}\rho(x,y,z)dEdxdy, \qquad (1)$$

where the xy plane coincides with the interface and the z direction is along the interface normal, A is the basal area of interface supercell. The calculated charge density profile is shown as a function of z in Fig. 4. Apart from the oscillations around the atom cores, the charge density decreases exponentially inside the oxide, with a decay length of λ_{ZrO_2} $\sim$0.9 Å which is nearly independent of the type of the metal and should be viewed as a property of c-ZrO_2 bulk. This decay length is rather short compared to that in Si (3.0 Å) and GaAs (2.8 Å),[18] which is consistent with the relatively smaller Schottky pinning parameter (S) for high-κ oxides than for Si and GaAs in the MIGS model.[20,21] With the short decay length, MIGS is not expected to contribute considerably to the band alignment between the metal and high-κ oxide because the electrostatic potential from the interface dipole cannot be efficiently screened by MIGS.

The p-type Schottky barrier height (p-SBH) Φ_p was determined using the standard bulk-plus-lineup[22,23] approach, with the average electrostatic potential at the ion core (V_{core}) in the "bulk" region as reference energy

$$\Phi_p = \Delta E_b + \Delta V, \qquad (2)$$

where ΔE_b is the difference between the Fermi energy of Ni and the energy of the valence band maximum (VBM) of the

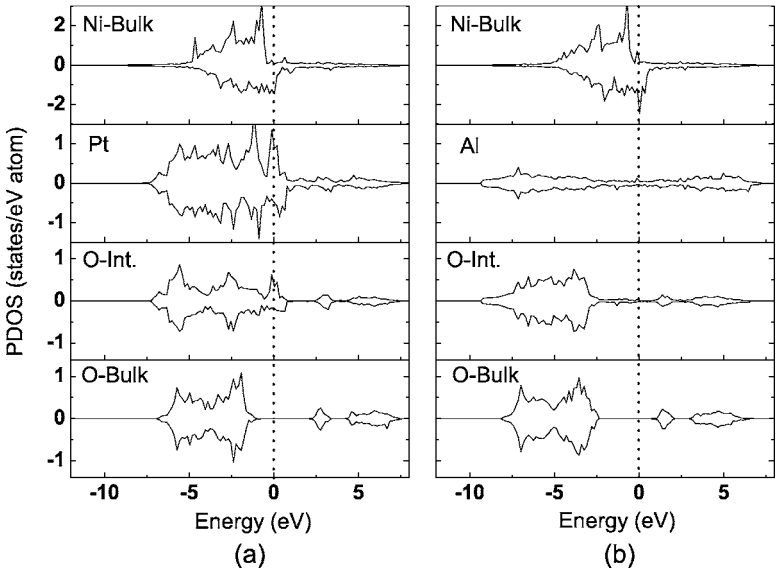

FIG. 3. Spin resolved and atomic site-projected density of states (PDOS) for (a) Ni-Pt-ZrO_2 interface and (b) Ni-Al-ZrO_2 interface, with half monolayer of metal insertion. The PDOS for the Ni in the bulk region (Ni-bulk), interface metal m (Pt or Al), interface oxygen (O-int), and oxygen in the bulk region (O-bulk) are shown.

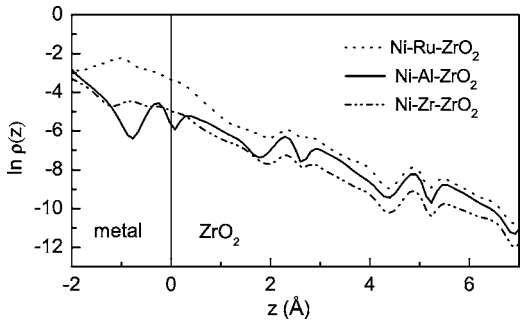

FIG. 4. Penetration of electronic density $\rho(z)$ of the gap states into the ZrO_2 of Ni-m-ZrO_2 (m=Ru,Al,Zr) interfaces. Position of the surface oxygen is set to z=0 Å. The penetration profiles for other Ni-m-ZrO2 interfaces are similar and are not shown.

oxide, each measured relative to V_{core} of the corresponding "bulk" ions, and ΔV is the lineup of V_{core} through the interface.

The average electrostatic potential V_{core} of Ni and Zr ions in the Ni-m-ZrO_2 interfaces are shown as a function of distance from the interface in Fig. 5. The V_{core} of the Ni ions near the interface were perturbed by the interface dipole, but quickly recovered its value in bulk region. On the oxide side, V_{core} for Zr ions have converged to its bulk value at the second Zr layer which is consistent with the short decay length of MIGS in ZrO_2. ΔV was evaluated from the difference in V_{core} of the Zr and Ni ions in their respective bulk regions.

The p-SBHs (Φ_p) were calculated from Eq. (2) for various Ni-m-ZrO_2 interfaces using the calculated ΔV and the quasiparticle[24,25] and spin-orbital corrected ΔE_b. The n-SBH (Φ_n) was derived from $\Phi_n = E_g - \Phi_p$, where E_g is the energy gap of the dielectric. The experimental band gap of 5.82 eV (Ref. 26) was used here instead of the DFT-GGA result because of the well-known underestimation of the latter. The

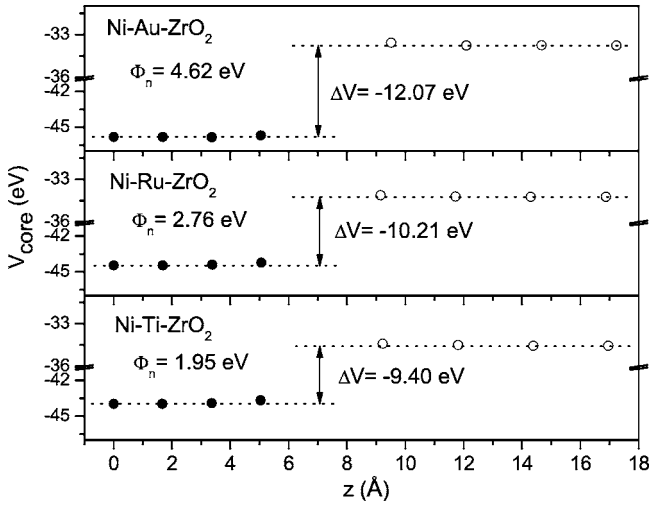

FIG. 5. Average electrostatic potential at the cores (V_{core}) of Ni (filled dark circle) and Zr (open circle) as a function of the distance from the interface for Ni-m-ZrO_2 interfaces (m=Au,Ru,Ti) with half monolayer metal insertion. Breaks were introduced in the vertical axis (V_{core}) between −41 and −36 eV.

TABLE I. Interface metal coverage (θ), electronegativity (Ref. 31) of metal atom m (χ, Mulliken scale, in eV), work function (Ref. 32) of metal m in vacuum ($\Phi_{m,\text{vac}}$, in eV), Mulliken charge (Q_m, in e), n-SBHs (Φ_n, in eV) for Ni-m-ZrO_2 interfaces, and effective metal work functions ($\Phi_{m,\text{eff}}$, in eV) for Ni-m-ZrO_2-Si capacitors.

m	θ	χ	$\Phi_{m,\text{vac}}$	Q_m	Φ_n	$\Phi_{m,\text{eff}}$
Au	0.5	5.77	5.1	0.16	4.62	6.92
Pt	0.5	5.6	5.65	0.16	3.84	6.14
Ni	0.5	4.4	5.15	0.37	2.76	5.06
Ru	0.5	4.5	4.71	0.27	2.76	5.06
Mo	0.5	3.9	4.6	0.51	2.38	4.68
Al	0.5	3.23	4.28	1.06	2.18	4.48
V	0.5	3.6	4.3	0.69	2.09	4.39
Zr	0.5	3.64	4.05	1.01	1.96	4.26
Ti	0.5	3.45	4.33	0.8	1.95	4.25
W	0.5	4.4	4.55	0.15	1.8	4.1
Ni	1	4.4	5.15	0.24	3.63	5.93
V	1	3.6	4.3	0.44	2.65	4.95
Al	1	3.23	4.28	0.63	1.82	4.12

effective metal work function ($\Phi_{m,\text{eff}}$) on the oxide was evaluated using the formula $\Phi_{m,\text{eff}} = \Phi_n - \text{CBO} + \text{EA}$, where CBO is the conduction band offset between the oxide and Si substrate (1.75 eV from Ref. 26) and EA is the electron affinity of Si (4.05 eV). Mulliken charges (in Table I) for interface metal m were calculated using Cambridge sequential total energy package (CASTEP).[27]

The calculated n-SBHs and effective metal work functions are listed in Table I for the Ni-m-ZrO_2 interfaces with various interlayer metals. The corresponding Fermi levels of metal gate electrodes in Ni-m-ZrO_2-Si capacitors (the coverage of interlayer metal m is 0.5.) were also depicted in Fig. 1. It can be seen that a tunability as wide as 2.8 eV for Φ_n ($\Phi_{m,\text{eff}}$) can be achieved for Ni-m-ZrO_2 interfaces by simply introducing half or one monolayer of heterovalent metal m between Ni and ZrO_2. Furthermore, we found that n-SBHs and effective metal work functions follow a crude chemical tuning trend: for a given metal m coverage (half or one monolayer), the n-SBH (effective work function) increases linearly with the electronegativity (χ) of the interlayer metal atom m. The effective work function data for the Ni-ZrO_2-Si MOS structures with half monolayer of metal m between Ni and ZrO_2 were fitted to a straight-line, as shown in Fig. 6. The simple linear relationship between $\Phi_{m,\text{eff}}$ and χ is obeyed by most transition metals except Al and W. The exceptional case of Al is probably due to its simple metal character (s and p valence electrons), in contrast to the transition metals (including d valence electrons). But reason is not clear for the exceptional behavior of tungsten.

The above linear chemical tuning trend is likely due to the localized interfacial dipole formed by different interfacial chemical bonds. Because of the short decay length (0.9 Å) of MIGS in ZrO_2, the localized interface dipole formed by interfacial polarized bonds plays a dominating role compared to MIGS in the formation of Schottky barrier heights for the metal-dielectric oxide interfaces. We may regard the inter-

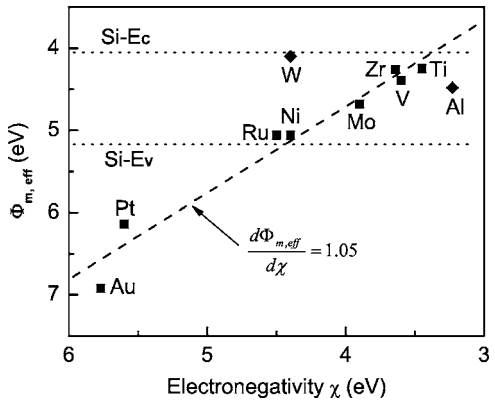

FIG. 6. Effective work functions ($\Phi_{m,\mathrm{eff}}$) of Ni-ZrO_2-Si structures with half monolayer of heterovalent metal *m* between Ni and ZrO_2 are shown as a function of electronegativity of interlayer metal *m*. The straight line is a least-square fit to data points shown in filled squares (Al and W are not included). The Si conduction band edge (E_C) and valence band edge (E_V) are at 4.05 and 5.17 eV, respectively.

face region as a large "molecule"[28] which connects the Ni bulk reservoir on one side and ZrO_2 bulk reservoir on the other side, so that the Ni-*m*-ZrO_2 interface takes the form of (Ni-bulk)-Ni-*m*-O-(ZrO_2-bulk), with -Ni-*m*-O- being the interface specific region. The interface dipole comprises two parts, one from the ionic *m*-O bonds, the other from the positively charged metal layer and its image charge in the metal (Ni) side. The former raises all energy levels on the oxide side with respect to the values in the metal, thus increases *n*-SBH, while the latter decreases *n*-SBH. With decreasing electronegativity of *m*, both types of dipole increase. But *n*-SBH decreases which indicates that the net interface dipole is pointing from the metal to the oxide, and the dipole formed by the *m* cation layer and its image charge plays the dominant role in determination of SBH. This may be the basis for observed chemical tuning trend. The above argument is only based on a phenomenal electrostatic model. We note that without detailed knowledge of the charge redistribution profile, and the microscopic dielectric constant at the interface, the shift of SBH cannot be derived exactly from electrostatic models, although such shift has been obtained self-consistently in our first-principles calculations.

Recently, Chiang *et al.*[29] demonstrated chemical tuning of metal-Si interfaces by measuring SBHs with angle-resolved photoemission. The chemical tuning trend for SBHs of metal-Si interfaces obtained in their study is the same as what we found here for metal-dielectric oxide interfaces, thus lending supports to our finding that interface dipole formed by interfacial metal cation layer and its image charge in the metal plays an important role in the formation of Schottky barrier height. However, the dependence of SBH on electronegativity of interfacial metal is much weaker for metal-Si interfaces than for metal-ZrO_2 interfaces, which may be due to the efficient MIGS screening of Si substrate.

In addition to the chemical effects, structural effects, such as interfacial metal *m* coverage, also play important roles in determining Schottky barrier heights. Ni-*m*-ZrO_2 interfaces with one monolayer coverage of Al, V and Ni were investigated similarly. The results shown in Table I indicate that SBH also strongly depends on interfacial structure.

For a comparison of our results with experiments, a few cautions should be borne in mind. The model assumes that heterovalent metal atoms form a complete layer between the metal electrode and high-κ oxide, which is a very restrictive condition. Real metal/metal-oxide interface structures should be deposition-process-dependent and there would be many disorders or defects at real metal/metal-oxide interfaces. For example, oxygen-rich or -deficient conditions result in different surface[30] or interface structures;[9] diffusion or aggregation of the interfacial heterovalent metal atoms may be expected at elevated temperature or even at room temperature. The resulting compositional and morphological inhomogeneities will lead to charge rearrangement at the interface which may damp the expected chemical tuning effects.

IV. CONCLUSION

In conclusion, chemical tuning of the band alignment for Ni-ZrO_2 interfaces by introducing heterovalent metal interlayer has been studied using first-principles DFT calculations. A remarkable tuning range (2.8 eV) for effective metal work function ($\Phi_{m,\mathrm{eff}}$) was achieved theoretically. Furthermore, a general chemical tuning trend was established for most of the transition metals considered, that is, $\Phi_{m,\mathrm{eff}}$ increases linearly with the electronegativity of the interfacial metal atom. Although the complicated situations in real metal gate/dielectric oxides interfaces limit the predictive power of our results, the simple linear relationship between $\Phi_{m,\mathrm{eff}}$ and the electronegativity of interfacial metal atom would provide a valuable guide in tuning the effective work function of metal gate on high-κ dielectric.

*Electronic address: sj-wang@imre.a-star.edu.sg
†Electronic address: phyfyp@nus.edu.sg

[1] The International Technology Roadmap for Semiconductor 2004, URL: http://public.itrs.net
[2] G. D. Wilk, R. M. Wallace, and J. M. Anthony, J. Appl. Phys. **89**, 5243 (2001).
[3] S. J. Wang and C. K. Ong, Appl. Phys. Lett. **80**, 2541 (2002).
[4] P. W. Peacock and J. Robertson, Phys. Rev. Lett. **92**, 057601 (2004).
[5] C. J. Först, C. R. Ashman, K. Schwarz, and P. E. Blöchl, Nature (London) **427**, 53 (2004).
[6] Y. F. Dong, Y. P. Feng, S. J. Wang, and A. C. H. Huan, Phys. Rev. B **72**, 045327 (2005).
[7] Yee-Chia Yeo, Tsu-Jae King, and Chenming Hu, J. Appl. Phys. **92**, 7266 (2002).
[8] V. V. Afanas'ev, M. Houssa, A. Stesmans, and M. M. Heyns, J.

Appl. Phys. **91**, 3079 (2002).
[9] Y. F. Dong, S. J. Wang, J. W. Chai, Y. P. Feng, and A. C. H. Huan, Appl. Phys. Lett. **86**, 132103 (2005).
[10] Seongjun Park, Luigi Colombo, Yoshio Nishi, and Kyeongjae Cho, Appl. Phys. Lett. **86**, 073118 (2005).
[11] I. De, D. Johri, A. Srivastava, and C. M. Osburn, Solid-State Electron. **44**, 1077 (2000).
[12] A. A. Knizhnik, I. M. Iskandarova, A. A. Bagatur'yants, B. V. Potapkin, and L. R. C. Fonseca, J. Appl. Phys. **97**, 064911 (2005).
[13] G. Kresse and J. Hafner, Phys. Rev. B **47**, R558 (1993); **48**, 13115 (1993).
[14] G. Kresse and J. Furthmuller, Comput. Mater. Sci. **6**, 15 (1996); Phys. Rev. B **54**, 11169 (1996).
[15] D. Vanderbilt, Phys. Rev. B **41**, R7892 (1990).
[16] J. P. Perdew, J. A. Chevary, S. H. Vosko, K. A. Jackson, M. R. Pederson, D. J. Singh, and C. Fiolhais, Phys. Rev. B **46**, 6671 (1992).
[17] Peter E. Blöchl, O. Jepsen, and O. K. Andersen, Phys. Rev. B **49**, 16223 (1994).
[18] S. G. Louie, J. R. Chelikowsky, and M. L. Cohen, Phys. Rev. B **15**, 2154 (1977).
[19] J. Tersoff, Phys. Rev. Lett. **52**, 465 (1984).
[20] John Robertson, J. Vac. Sci. Technol. B **18**, 1785 (2000).
[21] Winfried Mönch, Appl. Phys. Lett. **86**, 122101 (2005).
[22] M. Peressi, N. Binggeli, and A. Baldereschi, J. Phys. D **31**, 1273 (1998).
[23] S. H. Wei and A. Zunger, Phys. Rev. Lett. **59**, 144 (1987).
[24] B. Králik, E. K. Chang, and S. G. Louie, Phys. Rev. B **57**, 7027 (1998).
[25] V. Fiorentini and G. Gulleri, Phys. Rev. Lett. **89**, 266101 (2002).
[26] S. J. Wang, A. C. H. Huan, Y. L. Foo, J. W. Chai, J. S. Pan, Q. Li, Y. F. Dong, Y. P. Feng, and C. K. Ong, Appl. Phys. Lett. **85**, 4418 (2004).
[27] M. D. Segall, P. L. D. Lindan, M. J. Probert, C. J. Pickard, P. J. Hasnip, S. J. Clark, and M. C. Payne, J. Phys.: Condens. Matter **14**, 2717 (2002).
[28] R. T. Tung, Phys. Rev. Lett. **84**, 6078 (2000).
[29] D. A. Ricci, T. Miller, and T.-C. Chiang, Phys. Rev. Lett. **93**, 136801 (2004).
[30] Andreas Eichler and Georg Kresse, Phys. Rev. B **69**, 045402 (2004).
[31] R. G. Pearson, Inorg. Chem. **27**, 734 (1988); R. S. Mulliken, J. Chem. Phys. **2**, 782 (1934).
[32] H. B. Michaelson, J. Appl. Phys. **48**, 4729 (1977).